

Concluding Remarks

The adsorption equation for homogeneous surface, Eq. (1), can represent single-component isotherms of hydrocarbons and carbon dioxide on activated fiber carbon KF-1500 fairly well, but systematic deviations were observed in regions of low surface coverage. The total amount of active sites W^\bullet may be an adsorbent property which is proportional to the specific surface area. The value of W^\bullet for KF-1500 is 33% greater than that of Nuxit-AL, an activated granular carbon. The obtained parameters n and K are almost the same for the two activated carbons.

The isosteric heats of adsorption calculated from the experimental isotherms decrease with increasing surface coverage for the five adsorbates on KF-1500. The curves of the isosteric heat indicate that the surface is a little heterogeneous. These observations are compatible with systematic deviations between the calculated and the experimental adsorptions.

Acknowledgment

The authors are grateful to Toyobo Co., Ltd. for providing the activated fiber carbon KF-1500.

Nomenclature

A_p	= molecular cross-sectional area	[nm ²]
K	= adsorption equilibrium constant	[Pa ⁻¹]
M	= molar mass	[g·mol ⁻¹]
n	= number of sites occupied by a molecule	[—]
P	= pressure	[Pa]
Q_{st}	= isosteric heat of adsorption	[J·mol ⁻¹]
T	= temperature	[K]
W	= amount adsorbed per gram of adsorbent	[mol·g ⁻¹]
W^\bullet	= amount of sites per gram of adsorbent	[mol·g ⁻¹]
θ	= surface coverage	[—]

Literature Cited

- 1) Nitta, T., T. Shigetomi, M. Kuro-oka and T. Katayama: *J. Chem. Eng. Japan*, **17**, 39 (1984).
- 2) Szepeszy, L. and V. Illés: *Acta Chim. Hung.*, **35**, 37 (1963); *Acta Chim. Hung.*, **35**, 53 (1963).

BUBBLE FORMATION PATTERN WITH WEEPING AT A SUBMERGED ORIFICE

TOSHIRO MIYAHARA, MINORU IWATA AND TERUO TAKAHASHI
Department of Industrial Chemistry, Okayama University, Okayama 700

Key Words: Fluid Mechanics, Bubble Formation Regime, Weeping, Single Orifice, Transitional Point

Bubble formation phenomena with weeping at a submerged orifice were investigated experimentally over a range of orifice diameters of 3–13.2 mm. There appeared to be four regimes of interest: single bubbling at small chamber volumes and low gas flow rates, doubling noticed with increasing gas flow rate, jetting at further increase of gas flow rate and pairing at very large chamber volumes under conditions of gas flow rates smaller than those for jetting point. Empirical relationships predicting each transitional point of bubble formation regimes are obtained.

Introduction

Gas-liquid contacting devices such as bubble and plate columns are very widely used for the transfer of matter or heat across an interface in the chemical industry. In such devices perforated plates, which serve for the dispersion of gases, have been widely used because of their simple structure.

As is well-known, weeping through the perforations of perforated plates, usually undesirable, occurs with relatively large hole diameters and low gas flow rates during bubble formation.^{2,7)} It does not

occur on plates with small hole diameters and operation at very large gas flow rates.

To clarify the gas-liquid contacting mechanism, the phenomena of bubble formation from single holes have been extensively studied. Numerous studies have been made of the formation of gas bubbles under conditions where weeping has not occurred.^{3,6)}

McCann *et al.*⁴⁾ have studied bubble volume and weeping rate theoretically, using potential flow analysis. However, in their work, supporting data were presented for the air-water system only in the range of large gas flow rates where the phenomena of pairing or doubling mentioned below might occur. More recently, Akagi *et al.*¹⁾ have examined the

Received March 23, 1984. Correspondence concerning this article should be addressed to T. Miyahara. M. Iwata is now with Kao Corporation, Tokyo 103.

phenomena of weeping from a single orifice of 5 mm diameter with a chamber volume of 2000 cm³ in detail by means of high-speed motion pictures. But their work is not concerned with bubble formation, the phenomena of which are very important for the design or the operation of gas-liquid contacting devices with perforated plate. Therefore, it is necessary to know the bubble formation pattern with weeping.

In the present paper, bubble formation with weeping from a single orifice was experimentally studied over a wide range of orifice diameters, chamber volumes and physical properties of liquid. The appearance of four regimes of bubble formation with weeping was noticed and each transitional point of bubble formation regimes is made clear.

1. Experimental

Figure 1 is a schematic diagram of the experimental apparatus. The test section ⑬ comprised a 20 × 20 × 46 cm, transparent acrylic, right-angled parallelepiped. The orifices used were made of brass plate. Details of the geometry are given in **Table 1**. Most of the experiments were conducted by using orifices with a thickness of 1 mm.

Air from the compressor ① flowed through the filter ② the pressure regulator ③, the buffer tank ④ to suppress the pressure fluctuation, the orifice flow meter ⑥ or the rotameter ⑦ (Kusano Kagaku KG-70) and the capillary into the gas chamber ⑪, whose volume changed from 75 to 14,000 cm³. It then passed through the orifice ⑫, being dispersed in the liquid in the form of bubbles. The bubble frequency was measured by means of the light ⑱, the phototransistor ⑲, the preamplifier ⑳ and the digital counter ㉑ (Takeda Riken TR-5735).

Weeping liquid was collected by the funnel ⑭ beneath the plate and its weeping rate was measured as overflow rates from the constant-head tank ⑮. To eliminate the decrease of liquid level above the plate due to weeping and maintain a constant level, the different constant-head tank ⑯ was installed.

Bubble formation and weeping were photographed with the aid of a Hycam 100 FT model high-speed camera (400–1000 frames/s).

Table 2 lists the physical properties of the liquids employed: water, aqueous ethanol solutions, aqueous millet jelly solutions and aqueous glycerine solution. All experiments were carried out with a liquid depth of 20 cm.

2. Results and Discussion

2.1 Bubble formation pattern

Liquid weeping through an orifice usually occurs for large hole diameters after the detachment of a bubble. **Figure 2** shows a schematic diagram of four different bubble formation regimes with weeping:

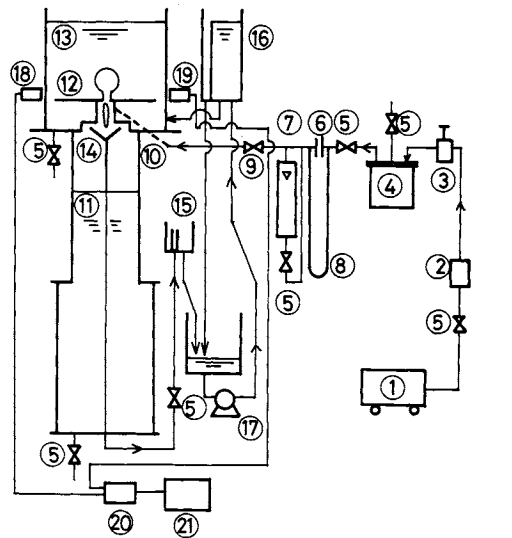


Fig. 1. Schematic diagram of experimental apparatus. 1, air compressor; 2, air filter; 3, pressure regulator; 4, buffer tank; 5, valve; 6, orifice flow meter; 7, rotameter; 8, manometer; 9, needle valve; 10, capillary; 11, gas chamber; 12, orifice; 13, test section; 14, funnel; 15, constant-head tank; 16, constant-head tank; 17, pump; 18, light; 19, phototransistor; 20, amplifier; 21, digital counter.

Table 1. Geometries of orifices

Orifice No.	$d_o \times 10^2$ [m]	$p_t \times 10^2$ [m]	p_t/d_o [—]
1	1.32	0.10	0.0756
2	1.10	0.10	0.0909
3	0.70	0.10	0.143
4	0.40	0.10	0.250
5	0.30	0.10	0.333

Table 2. Physical properties of liquids employed

Liquid	ρ_l [kg/m ³]	μ_l [Pa·s]	σ [N/m]
Water	1000	0.001	72.0×10^{-3}
Aqueous ethanol soln. 1	969	0.00255	37.2×10^{-3}
Aqueous ethanol soln. 2	953	0.00261	35.6×10^{-3}
Aqueous ethanol soln. 3	964	0.00271	35.1×10^{-3}
Aqueous millet jelly soln. 1	1263	0.0410	70.7×10^{-3}
Aqueous millet jelly soln. 2	1257	0.0353	71.4×10^{-3}
Aqueous millet jelly soln. 3	1308	0.135	66.5×10^{-3}
Aqueous glycerine soln.	1196	0.0356	60.8×10^{-3}

single bubbling, doubling, pairing and jetting observed in the present experiments. The detailed high-speed motion pictures for single bubbling are shown in **Fig. 3**. Thus, in single bubbling, where chamber volumes are small and gas flow rates are low, initially an almost spherical bubble is formed at an orifice, proceeds to grow a neck and then becomes detached. That is, the growth of the bubble is a two-stage process and weeping does not occur during bubble formation, but occurs after the detachment of the bubble. **Figure 4** shows the details of the doubling. In

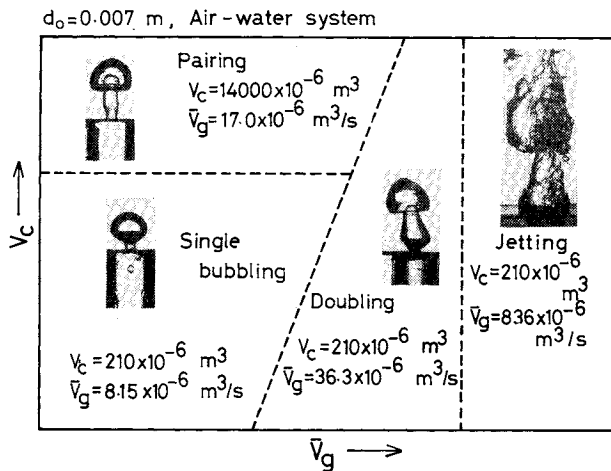
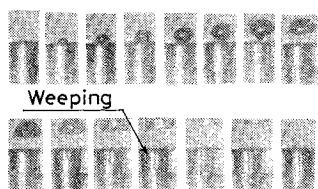
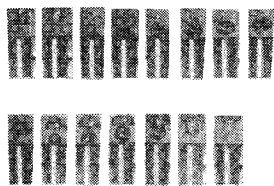


Fig. 2. Schematic diagram showing bubble formation patterns.



Single bubbling, Air-water system
 $V_c=2000 \times 10^{-6} \text{ m}^3$, $d_o=0.007$ m
 $\bar{V}_g=14.4 \times 10^{-6} \text{ m}^3/\text{s}$

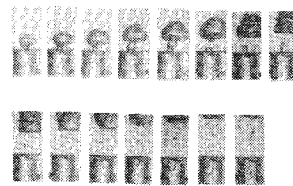
Fig. 3. Bubble formation in single bubbling regime.



Doubling, Air-water system
 $V_c=210 \times 10^{-6} \text{ m}^3$, $d_o=0.007$ m
 $\bar{V}_g=36.3 \times 10^{-6} \text{ m}^3/\text{s}$

Fig. 4. Bubble formation in doubling regime.

the doubling, where gas flow rates are relatively large and chamber volumes are small, coalescence with a new bubble generated at an orifice occurs immediately after the preceding bubble detaches itself from the orifice. Weeping, which does not show liquid column or drop but creeping flow along the underside of the orifice, occurs after the detachment of the coalesced bubble. The details of the pairing are shown in Fig. 5. At low and moderate gas flow rates in the case of very large chamber volumes, pairing with coalescence occurring in such a way that the preceding bubble expands by forming a tail takes place at all times and weeping still occurs after the detachment of the coalesced bubble. However, very large gas flow rates cause jetting, where weeping does not occur regardless



Pairing, Air-water system
 $V_c=14000 \times 10^{-6} \text{ m}^3$, $d_o=0.007$ m
 $\bar{V}_g=25.2 \times 10^{-6} \text{ m}^3/\text{s}$

Fig. 5. Bubble formation in pairing regime.

Air-aqueous millet jelly soln. 1 system



$V_c=460 \times 10^{-6} \text{ m}^3$, $d_o=0.011$ m, $\bar{V}_g=16.0 \times 10^{-6} \text{ m}^3/\text{s}$

Fig. 6. Synchronous phenomenon of bubble formation and weeping.

of chamber numbers, and the surface of the jet is not smooth.

As mentioned above, generally speaking, weeping occurs immediately after the detachment of a bubble. As shown in Fig. 6, however, orifices with large hole diameters sometimes cause both bubble formation and weeping simultaneously in the single bubble formation regime. The cause of this phenomenon could not be found in the present experiments because of their complexity. Therefore, only the bubble formation phenomena except for those shown in Fig. 6 will be considered here.

2.2 Transitional points in bubble formation

1) Transition from single bubbling to doubling
 Now that we have shown the patterns of bubble formation with weeping, we must ascertain each transitional point of bubble formation regimes. A stroboscope was used to determine the point of the single bubbling-to-doubling transition for various orifice diameters, physical properties of liquid and chamber volumes. In the authors' previous paper,⁵⁾ which described bubble formation at high gas flow rates, the coalescence of bubble was found to depend on the orifice diameter, the chamber number N_c ⁶⁾ and the physical properties of liquid. However, in this case the effect of viscosity was not noticed. There the dimensional analysis for the transition gave

$$f(We, Bo, N_c) = 0 \quad (1)$$

where $We = \rho_1 U_g^2 d_o / \sigma$, $Bo = \rho_1 g d_o^2 / \sigma$ and $N_c = 4V_c \Delta \rho g / \{\pi d_o^2 (P_o + \rho_1 g h)\}$. Figure 7 shows the correlation of the point of the single bubbling-to-doubling transition on the basis of Eq. (1) where k' involved in the ordinate is a function of Bo . The value of k' is given

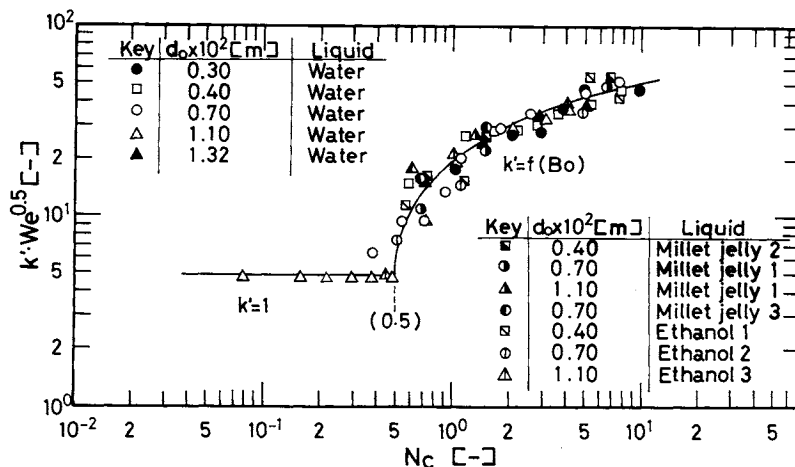


Fig. 7. Correlation of transitional points from single bubbling to doubling.

by Fig. 8. As is apparent from these figures, Weber numbers for the transitional points depend on N_c and Bo in $N_c > 0.5$, whereas they are independent of N_c and Bo in $N_c < 0.5$. This is presumably because of the small pressure fluctuation in the chamber for $N_c < 0.5$. The value of k' is given for $N_c > 0.5$ by the expressions,

$$\left. \begin{aligned} k' &= 1 & Bo < 13 \\ k' &= 0.0163Bo^{1.67} & 13 < Bo < 23 \\ k' &= 3 & 23 < Bo \end{aligned} \right\} \quad (2)$$

2) Transition from single bubbling to pairing The single bubbling-to-pairing transition was also determined by use of a stroboscope. The transitional points were found to be affected mainly by the orifice diameter d_0 and the chamber number N_c , unlike the single bubbling-to-doubling transition. Therefore, Fig. 9 shows the correlation of the single bubbling-to-pairing transition. The data in the figure show those for the transition from single bubbling to pairing. The solid line in this figure shows the perfect transition from pairing to single bubbling, while the dashed line shows that from single bubbling to pairing. Although the transition shows the broad region noticed in Fig. 9, we will take the solid line as the transitional point.

3) Transition from doubling to jetting The doubling-to-jetting transition was taken as the point at which weeping did not occur. Figure 10 shows an example of weeping rates. Roughly speaking, it is noticed that liquid velocity through a hole which corresponds to weeping rate for small values of N_c , increases with gas velocity through a hole, gives two maximum values, then decreases with gas velocity and finally reaches zero where weeping does not occur, whereas liquid velocity for large values of N_c shows one maximum value. In any case, however, liquid velocity increases with increasing chamber number N_c at first and then decreases with further increase of N_c ,

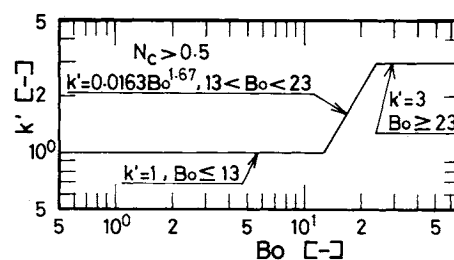


Fig. 8. Correction factor k' .

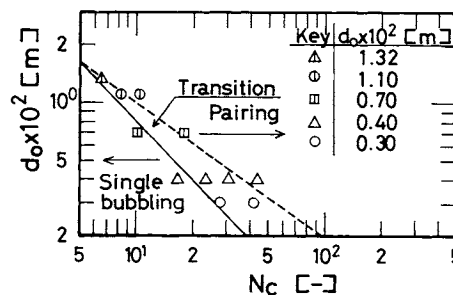


Fig. 9. Correlation of transitional points from single bubbling to pairing.

which is not shown here. It seems that the existence of one or two maximum values is comparable to the bubble formation pattern, although the cause of the details is unknown. As can be seen from this figure, the weeping phenomena are very complex. Then, we will try to correlate points of the doubling-to-jetting transition according to the authors' previous results.⁵⁾ There the dimensional analysis for the transition gave a function of the Weber number and the Bond number as

$$f(We, Bo) = 0 \quad (3)$$

Figure 11 shows the relationship between the Weber number and the Bond number, based on the empirical data of the transition. The doubling-to-jetting transition is explained by the solid line, which shows a

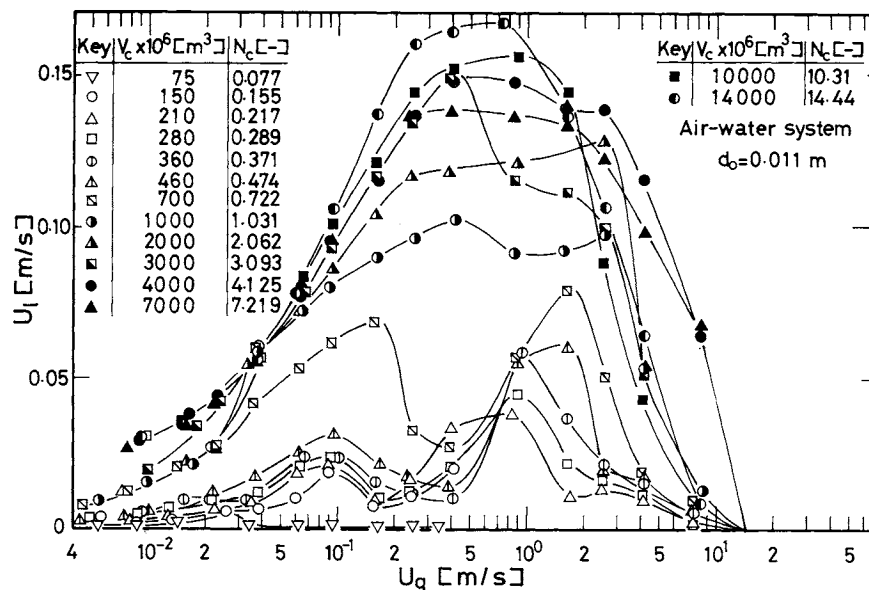


Fig. 10. Weeping rate.

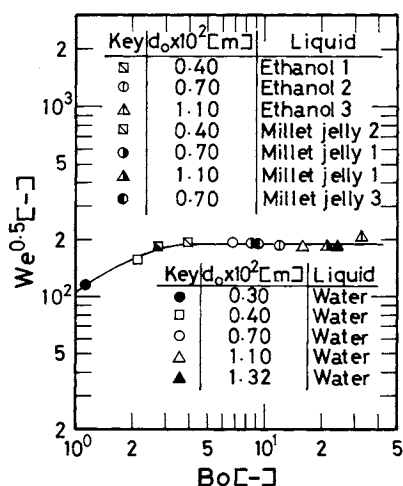


Fig. 11. Correlation of transitional points from doubling to jetting.

constant value at Bond numbers above roughly 4.

Accordingly, as one instance among many, we made Fig. 12 for $d_o = 0.004, 0.007$ and 0.011 m using the correlations for each transitional point shown in Figs. 7, 9 and 12. This figure shows the four different regimes of the bubble formation with weeping at single orifices.

Conclusion

Bubble formation with weeping at a single orifice was studied experimentally over a wide range of gas chamber volumes and physical properties of liquid by using orifices with relatively large hole diameters. The following results were remarked:

- 1) Four regimes of bubble formation of interest exist: single bubbling, doubling, pairing and jetting.
- 2) The relationships predicting the transitions

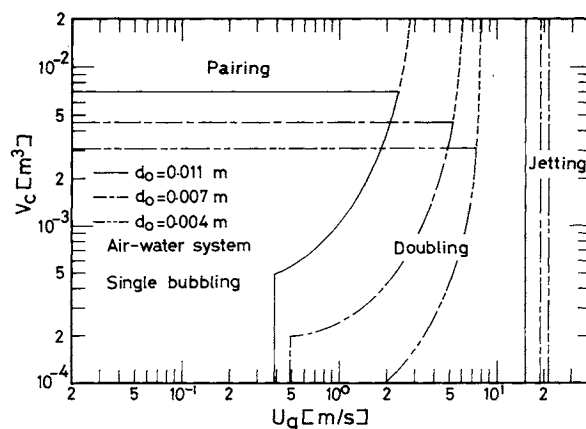


Fig. 12. State diagram showing regimes of bubble formation with weeping.

from single bubbling to doubling, single bubbling to pairing and doubling to jetting are obtained.

3) Liquid weeping through an orifice occurs immediately after the detachment of the bubble. However, orifices with large hole diameters sometimes show both bubble formation and weeping simultaneously. The criterion for this phenomenon could not be clarified in the present experiments.

Nomenclature

Bo	= Bond number = $\rho_l g d_o^2 / \sigma$	[—]
d_o	= orifice diameter	[m]
g	= gravitational acceleration	[m/s ²]
k'	= correction factor	[—]
N_c	= chamber number = $4V_c \Delta \rho g / \{\pi d_o^2 (P_o + \rho_l g h)\}$	[—]
P_o	= barometric pressure	[Pa]
P_i	= plate thickness	[m]
U_l	= weeping velocity through hole	[m/s]
U_g	= gas velocity through hole	[m/s]
V_c	= chamber volume	[m ³]

\bar{V}_g = mean volumetric gas flow rate into chamber [m^3/s]
 We = Weber number = $\rho_l U_g^2 d_o / \sigma$ [—]
 $\Delta\rho$ = $\rho_l - \rho_g$ [kg/m^3]
 μ_l = viscosity of liquid [$\text{Pa}\cdot\text{s}$]
 ρ_g, ρ_l = density of gas and liquid [kg/m^3]
 σ = surface tension [N/m]

Literature Cited

- 1) Akagi, Y. and T. Takahashi: *Kagaku Kogaku Ronbunshu*, **9**, 594 (1983).
- 2) Akagi, Y., M. Nishikaze, S. Yamamoto and T. Takahashi: *Kagaku Kogaku Ronbunshu*, **7**, 442 (1981).
- 3) Kumar, R. and N. R. Kuloor: "Advances in Chemical Engineering," **8**, 255 (1970).
- 4) McCann, D. J. and R. G. H. Prince: *Chem. Eng. Sci.*, **24**, 801 (1969).
- 5) Miyahara, T., N. Haga and T. Takahashi: *Intern. Chem. Eng.*, **24**, 524 (1983).
- 6) Tadaki, T. and S. Maeda: *Kagaku Kōgaku*, **27**, 147 (1963).
- 7) Zenze, F. A. L., L. Stone and M. Crane: *Hydrocarbon Processing*, **46**, 138 (1967).

BUBBLE VOLUME IN SINGLE BUBBLING REGIME WITH WEEPING AT A SUBMERGED ORIFICE

TOSHIRO MIYAHARA AND TERUO TAKAHASHI

Department of Industrial Chemistry, Okayama University, Okayama 700

Key Words: Fluid Mechanics, Bubble Volume, Weeping, Single Orifice, Two-Stage Model

Bubble volumes in the single bubbling regime, which is one of bubble formation regimes with weeping, are larger than those for bubble formation without weeping. A theoretical treatment for bubble formation with weeping is performed to predict bubble volume in the single bubbling regime where weeping through an orifice occurs after the detachment of a bubble, and a comparison with measurements is made.

Introduction

A number of gas-liquid contacting devices in the chemical industry contain perforated plates because of their simplicity. Recently, industrial operation requires plates having relatively large free areas, which correspond to large hole diameters, where weeping occurs. Therefore, knowledge of bubble formation with weeping is important for the design or operation of gas-liquid contacting devices with perforated plates.

To clarify the gas-liquid contacting mechanism, many investigators^{3-5,8,11,14,17,18)} have studied bubble formation at single holes. Less attention, however, has been given to bubble formation phenomena with weeping.

McCann *et al.*⁷⁾ have proposed a model to describe bubble volume and weeping rate theoretically using potential flow analysis, but they did not consider the effect of viscosity.

In a previous paper,⁹⁾ the authors observed four regimes of bubble formation with weeping based on operating conditions and orifice geometries: single

bubbling, doubling, pairing and jetting.

In the present paper, a theoretical treatment for bubble formation with weeping is given by using the previous two-stage model and is shown to be in fairly good agreement with measurements in the single bubble formation regime, which is one of the bubble formation regimes with weeping observed previously by the authors.⁹⁾

1. Experimental

The experimental apparatus and procedure used are the same as those described in the previous paper.⁹⁾

All of the orifices used with diameters of 3–13.2 mm were made of brass plate of 1 mm thickness ($p_i/d_o = 0.075$ – 0.33). Eight different liquids were studied: water, aqueous ethanol solutions, aqueous millet jelly solutions and aqueous glycerine solution. Experiments were carried out over a range of densities of 953–1263 kg/m^3 , a range of viscosities of 1×10^{-3} – 13.5×10^{-3} $\text{Pa}\cdot\text{s}$ and a range of surface tensions of 35.1×10^{-3} – 72.0×10^{-3} N/m . The details are shown in Table 1, which is the same as that in the previous paper.⁹⁾ Chamber volumes changed from 75 to 14,000 cm^3 .

Received March 23, 1984. Correspondence concerning this article should be addressed to T. Miyahara.